Proc. Natl. Acad. Sci. USA
Vol. 74, No. 8, pp. 3171–3175, August 1977
Biochemistry

Spliced segments at the 5′ terminus of adenovirus 2 late mRNA*

(adenovirus 2 mRNA processing/5′ tails on mRNAs/electron microscopy of mRNA·DNA hybrids)

SUSAN M. BERGET, CLAIRE MOORE, AND PHILLIP A. SHARP

Center for Cancer Research and Department of Biology, Massachusetts Institute of Technology, Cambridge, Massachusetts 02139

Communicated by David Baltimore, May 9, 1977

ABSTRACT **An mRNA fraction coding for hexon polypeptide, the major virion structural protein, was purified by gel electrophoresis from extracts of adenovirus 2-infected cells late in the lytic cycle. The mRNA sequences in this fraction were mapped between 51.7 and 61.3 units on the genome by visualizing RNA·DNA hybrids in the electron microscope. When hybrids of hexon mRNA and single-stranded restriction endonuclease cleavage fragments of viral DNA were visualized in the electron microscope, branched forms were observed in which 160 nucleotides of RNA from the 5′ terminus were not hydrogen bonded to the single-stranded DNA. DNA sequences complementary to the RNA sequences in each 5′ tail were found by electron microscopy to be located at 17, 20, and 27 units on the same strand as that coding for the body of the hexon mRNA. Thus, four segments of viral RNA may be joined together during the synthesis of mature hexon mRNA. A model is presented for adenovirus late mRNA synthesis that involves multiple splicing during maturation of a larger precursor nuclear RNA.**

Most eukaryotic mRNAs bear modifications at both termini; their 3′ termini have a tract of poly(A) that ranges in length from 30 to 200 bases (1–4), while their 5′ termini are typically capped with a methylated guanine joined through a 5′-5′ pyrophosphate linkage to a second nucleotide methylated at its 2′ position (5, 6). Both types of modifications of eukaryotic mRNA are known to occur after transcription.

All adenovirus mRNAs are thought to contain poly(A) tracts at their 3′ termini (7) and be capped with a methylated guanine (8, 9). Specific restriction endonuclease cleavage fragments of adenovirus 2 (Ad2) DNA have permitted the mapping of regions of the genome expressed as mRNA and viral proteins during different stages of the lytic cycle (10–12). Little is known about the molecular mechanisms of viral mRNA synthesis. An important aspect of late mRNA synthesis is thought to be the processing and selection of viral mRNAs from the nucleus (13, 14). We have purified a late Ad2 hexon mRNA and found evidence providing some insight into the mechanism of synthesis of this mRNA.

MATERIALS AND METHODS

Isolation of Ad2 DNA and RNA. Polyribosomal RNA was prepared from Ad2-infected cells 32 hr after infection as described by Flint and Sharp (14, 15) and selected by chromatography on poly(U)-Sephadex (16).

R-Loop Mapping. The R-loop hybridization mixture was essentially that of Thomas *et al.* (17) and contained 70% (vol/vol) formamide [Matheson, Coleman, and Bell, 99%, further purified as described by Duesberg and Vogt (18)]; 0.20 M Tris·HCl, pH 7.91; 0.50 M NaCl; 0.01 M EDTA; Ad2 DNA at 10 μg/ml; and purified hexon mRNA at 1–10 μg/ml. This mixture was incubated at 52.5° for 2–3 hr and spread on a hypophase of water with internal length standards of DNA from bacteriophage φX174, 5375 bases (19).

Hybridization to Single-Stranded Ad2 DNA. Hybridizations of either polyribosomal poly(A) or purified hexon mRNA with restriction endonuclease fragments of Ad2 DNA were carried out in reaction mixtures of 80% formamide; 0.40 M NaCl; 0.04 M 2-(*N*-morpholino)ethanesulfonic acid (Mes), pH 6.2; 0.01 M EDTA; DNA at 10 μg/ml; and hexon mRNA at 1.0–10 μg/ml (20). The sample was incubated at 57–60° for 2–3 hr.

RESULTS

Adenovirus late mRNAs begin to appear on polyribosomes about 13 hr after infection and continue to accumulate in the cell throughout the lytic cycle (21). Thus, to fractionate the most abundant late mRNAs, polyribosomes were prepared from cells 32 hr after infection with Ad2 and poly(A)-containing mRNA was selected by chromatography on poly(U)-Sephadex columns. These mRNAs were then resolved into different molecular weight fractions by electrophoresis in 2.4–4.0% linear gradient polyacrylamide gels containing a uniform concentration of 7 M urea. After staining with ethidium bromide, distinct fluorescent bands were present in gels containing mRNA from virus-infected cells that were not found in gels containing identically prepared HeLa cell mRNA (Fig. 1*A*). These virus-specific RNAs were selectively labeled when [^{32}P]phosphate was added to infected cells 24 hr after infection and the same mRNA fractions were prepared (Fig. 1*B*). RNA from the predominant ethidium bromide-staining band migrating 1.5 times faster than 28S rRNA in Fig. 1*A* and marked with a large arrow has been shown to code for the hexon polypeptide by *in vitro* translation (S. M. Berget, B. E. Roberts, and P. A. Sharp, data not shown). Furthermore, this RNA has been mapped by the R-loop technique (see below) to a region of the genome known to code for hexon (12) and is complementary to the *r* strand of the viral DNA (11). This mRNA species, therefore, will be referred to in the following sections as hexon mRNA.

R-Loop Mapping of Hexon RNA. The R-loop technique developed by White and Hogness (22) and Thomas *et al.* (17) was used to position purified hexon mRNA on the viral genome. RNA eluted from a gel similar to that shown in Fig. 1*A* was incubated, as described in *Materials and Methods*, with either total Ad2 DNA or restriction endonuclease fragments. Of the 43 total Ad2 DNA molecules scored as containing R-loops, 41 were observed to have a single region of hybrid, while two molecules contain a second R-loop, apparently in the region of the genome coding for the 100K polypeptide (12).

Fig. 2 shows two examples of R-loops resulting from hybridization of hexon mRNA to fragments generated by the cleavage of Ad2 DNA with the *Eco*RI restriction endonuclease

The costs of publication of this article were defrayed in part by the payment of page charges from funds made available to support the research which is the subject of the article. This article must therefore be hereby marked "advertisement" in accordance with 18 U. S. C. §1734 solely to indicate this fact.

Abbreviation: Ad2, adenovirus 2.

* *We dedicate this work to the memory of Jerome Vinograd, a man who loved science.*

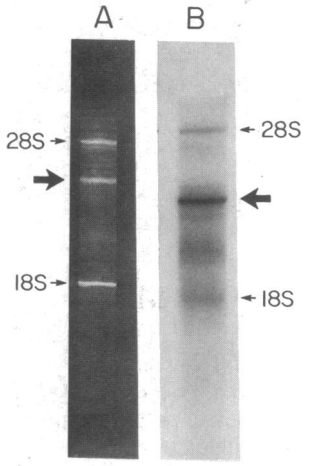

FIG. 1. Polyacrylamide gel electrophoresis of Ad2 mRNA. Polyribosomal poly(A)-containing RNA was prepared 32 hr after infection as described in *Materials and Methods* from either Ad2-infected cells (*A*) or infected cells to which [^{32}P]phosphate was added 24 hr after infection (*B*). Approximately 25 μg of this RNA was resolved by electrophoresis on 2.4–4.0% polyacrylamide gels containing 7 M urea for 16 hr at 100 V. The gel was either stained with 0.50 μg/ml of ethidium bromide and photographed (*A*) or autoradiographed (*B*).

(see Fig. 3 for fragment location). Hexon RNA spans the junction between the *Eco*RI A and B fragments, thus creating branches at one end of each fragment; one strand of the branch is single-stranded, the other is double-stranded and terminated in a ball of single-stranded RNA. Comparison of the lengths of the two hybrids with an internal standard of double-stranded ϕX174 DNA maps the 5′ end of the RNA at 51.7 ± 0.5 units (uncertainties are as indicated in ref. 19) of the genome and the 3′ end at 61.3 ± 0.5 units, in close agreement with other estimations based on both R-loop mapping with total cytoplasmic RNA (23, 24) and the viral polypeptide mapping of Lewis *et al.* (12).

When hexon mRNA was incubated under conditions to form R-loops with Ad2 DNA that had been cleaved with the *Hin*dIII restriction endonuclease, R-loops of the type shown in Fig. 4

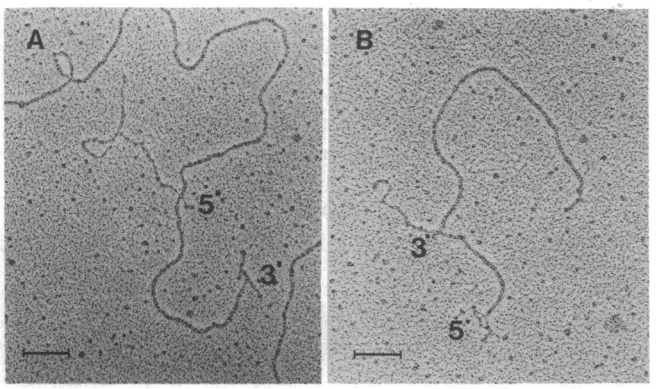

FIG. 2. R-Loops of purified hexon mRNA and *Eco*RI cleavage products of Ad2 DNA. Total Ad2 DNA cleaved by *Eco*RI and hexon mRNA were incubated and then spread to visualize R-loops as described in the *text*. Two examples of the 60 R-loop structures photographed and measured are shown; hydrid structures are observed at the ends of the *Eco*RI A fragment (*A*) and the *Eco*RI B fragment (*B*). The junction of these two fragments maps at 58.5 units on the Ad2 genome. The strand specificity of the mRNA sequences from this region (11) and the *Eco*RI cleavage map of Ad2 DNA were used to assign the 5′ and 3′ polarity of the RNA forming these R-loops. Bars represent 0.1 μm.

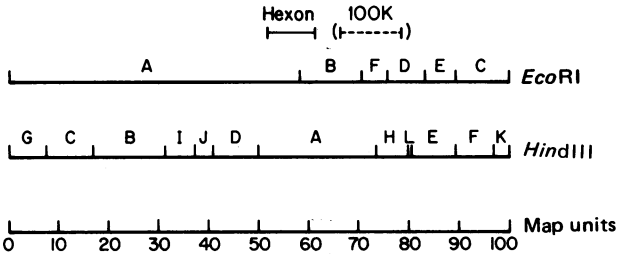

FIG. 3. Restriction map of Ad2 DNA. The vertical lines indicate the positions of cleavage for either the *Eco*RI or *Hin*dIII restriction endonucleases. The positions of genes coding for the hexon and 100,000 molecular weight (100K) polypeptides are from Lewis *et al.* (12).

A, *B*, and *C* were observed. The mRNA is totally included within the *Hin*dIII A fragment, forming R-loops terminating at positions 6.3 ± 0.1% and 50.2 ± 0.8% from the end of the fragment positioned at 50.1–73.6 map units on the Ad2 genome. Because hexon mRNA is known to be transcribed in the rightward direction (11), the map coordinates of hexon mRNA established from the R-loops to *Eco*RI fragments indicate that the 5′ end of hexon mRNA is 6.3% from the end of the *Hin*dIII A fragment. Small single-stranded "tails" were visible at both ends of the R-loop; such tails appeared on 88% of the 5′ ends (all polarities given with respect to the mRNA orientation) and on 75% of the 3′ ends of those R-loops with termini that mapped within two standard deviations of the mean position of the termini expected for full-length hybrids. Although the 3′ tail might in part be attributed to the poly(A) tracts of these mRNAs, the tail of the 5′ end of the mRNA was not expected and prompted further investigation.

Hybridization of Hexon RNA to Single-Stranded DNA. A possible interpretation of single-stranded tail-like structures at the ends of R-loops would be that branch migration creating DNA·DNA duplex had occurred, displacing the ends of the RNA (25). To examine this possibility, hybrids were formed with hexon mRNA and totally single-stranded *Hin*dIII A DNA. In such hybrids there would be no competing DNA·DNA renaturation to displace RNA·DNA hybrids. Such RNA·DNA hybrids were formed by incubating hexon mRNA with denatured *Hin*dIII A DNA at high formamide concentration (80%) and at 57° (20). After an appropriate incubation the hybrids were spread and examined under the electron microscope. As expected, little or no duplex *Hin*dIII A fragment was observed. Fig. 4 *D*, *E*, and *F* shows the types of hybrids that were observed with hexon mRNA and *Hin*dIII A DNA. Double-stranded hybrid segments were terminated with clearly visible tails at both the 5′ and 3′ ends of the mRNA molecules. Of those molecules having full-length hybrid, 90% had 5′ tails and 64% had 3′ tails. There may have been a bias in favor of selecting full-length hybrids with tails for screening because it was difficult to accurately position the ends of a duplex region that did not terminate in a forked structure. However, approximately 20% of the total *Hin*dIII A strands displayed a forked structure at the 5′-end position of the hexon mRNA. This result strongly suggests that the sequences in the tails are not complementary to the adjacent DNA sequences.

Histograms comparing the lengths of the hybrid regions observed in the R-loop technique to those produced by hybridization of hexon mRNA with denatured *Hin*dIII A DNA are shown in Fig. 5 *A* and *B*. When lengths are calculated from the hatched area of the histogram (those molecules containing full-length hexon RNA) the hybrid length is 3330 ± 290 base pairs for R-loop hybrids and 3540 ± 240 base pairs for hybrids formed with single-stranded *Hin*dIII A DNA. This agrees very

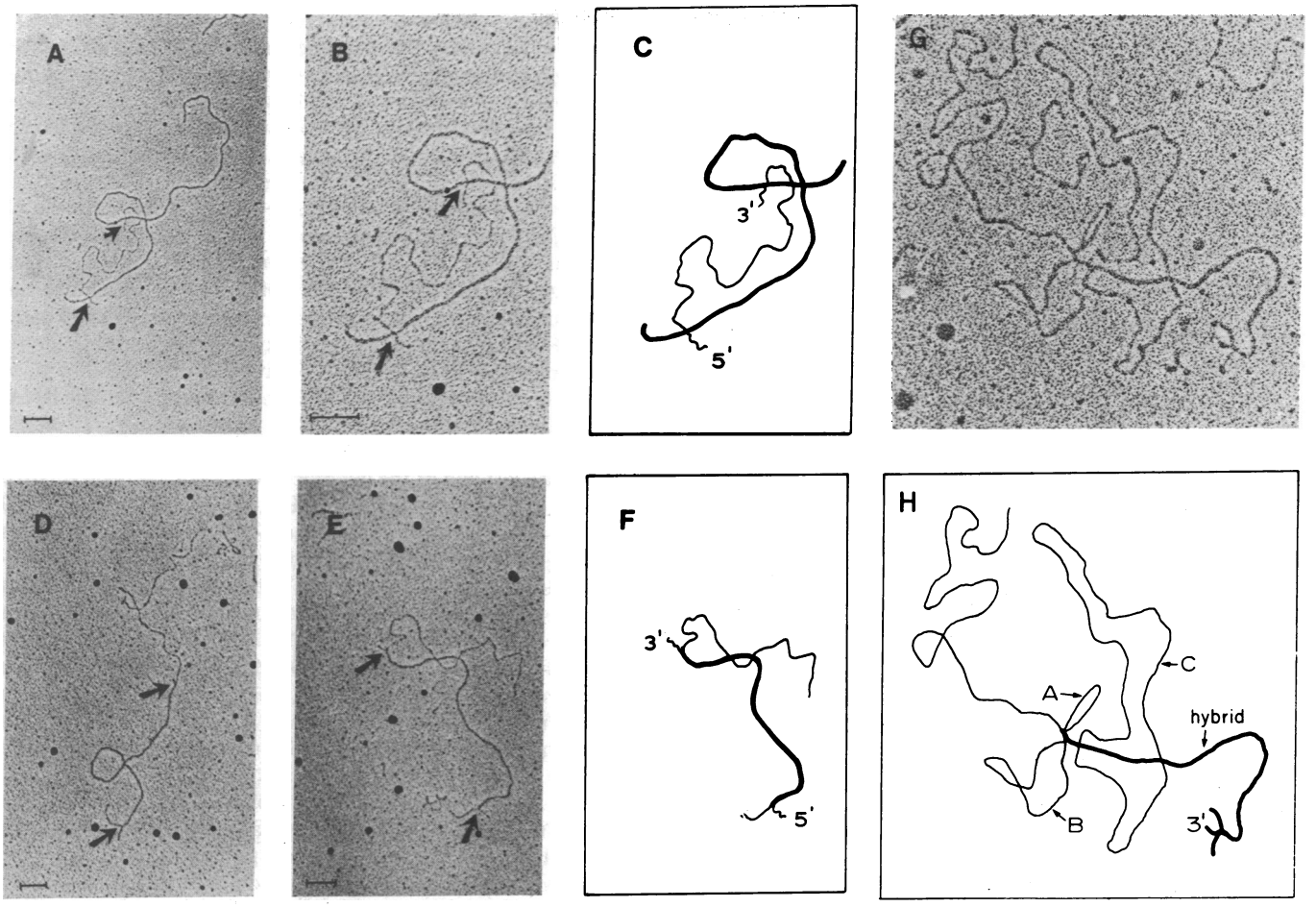

FIG. 4. Electron micrographs of hybrids of hexon mRNA and fragments of Ad2 DNA. An example of an R-loop hybrid observed after incubation of hexon mRNA and duplex *Hin*dIII A fragment DNA is shown in *A* and *B* and is diagrammed schematically in *C*. Similarly, two examples of hybrids of hexon mRNA and single-stranded *Hin*dIII A fragment are shown in *D* and *E*. A schematic of the hybrid structure shown in *E* is given in *F*. The single-stranded RNA at the end of the hybrid region is represented by a wave-like line. The hybrids of hexon mRNA and single-stranded *Hin*dIII A fragment DNA shown in *D* and *c* were mounted from an 80% formamide solution. In *A*, *B*, *D*, and *E* the positions of the RNA tails at the 5′ and 3′ ends of the hybrids are denoted by arrows. An example of a hybrid between single-stranded *Eco*RI A DNA and hexon RNA is shown in *G* and diagrammed in *H*. The hybrid region is indicated by a heavy line; loops A, B, and C (single-stranded unhybridized DNA) are joined by hybrid regions resulting from annealing of upstream DNA sequences to the 5′ tail of hexon mRNA. Bars on micrographs represent 0.1 μm.

well with the length of the RNA itself, 3510 ± 180 bases, as determined by visualization in the electron microscope following spreading by the urea/formamide technique (Fig. 5*C*) (26).

The measured lengths of 5′ and 3′ tails on the two types of hybrids are similar; the 5′ tails measure 170 ± 40 bases on R-loops and 160 ± 50 bases on hybrids with single-stranded DNA (Fig. 5 *D* and *E*); and the 3′ tail measures 150 ± 60 nucleotides on R-loops and 110 ± 40 nucleotides on hybrids with single-stranded DNA (Fig. 5 *F* and *G*). These contour lengths may be an underestimate because they were calculated assuming that single-stranded RNA chains were fully extended under the formamide spreading conditions employed. Those molecules having hybrids but no tails are also scored on the histograms in Fig. 5. In both techniques, those molecules having less than a full-length hybrid region were always missing at least one tail, suggesting that neither method artifactually generates such structures. Fig. 5 also contains two histograms showing the position of the 5′ tail with respect to the 50.1 unit end of the Ad2 *Hin*dIII A fragment (*H* and *I*); the 5′ tail appears to begin 480 ± 40 base pairs from the end of R-loop molecules and 410 ± 50 bases from an end of the hybrid molecules formed with the single-stranded *Hin*dIII A fragment.

The presence of branched structures suggested that the 5′ end of hexon mRNA may not be complementary to the adjacent region of DNA. Several alternate explanations remained to be eliminated by control experiments. The first involved the possibility that the branched structure was due to an unusually (A+T)-rich set of DNA sequences at this position which would be melted at the high formamide–high temperature spreading conditions employed. To eliminate this possibility, hybridization mixtures of hexon RNA and the purified denatured *Hin*dIII A fragment were diluted 70-fold into either 50% or 40% formamide solution and prepared for electron microscopy; under these conditions melting of even highly (A+T)-rich complementary sequences should not be observed. However, hybrid structures still contained 5′ and 3′ tails at the same frequency as those scored at the higher formamide concentrations (histogram not shown).

Another possibility was that the tails might arise from palindromic sequences at the ends of the mRNA molecules which were more stable as RNA·RNA hybrids and thus would not form hybrids with the complementary DNA. If such palindromic sequences were present in the Ad2 *Hin*dIII A fragment at this position, they should be visible as hairpins on single-stranded *Hin*dIII A DNA spread under low formamide

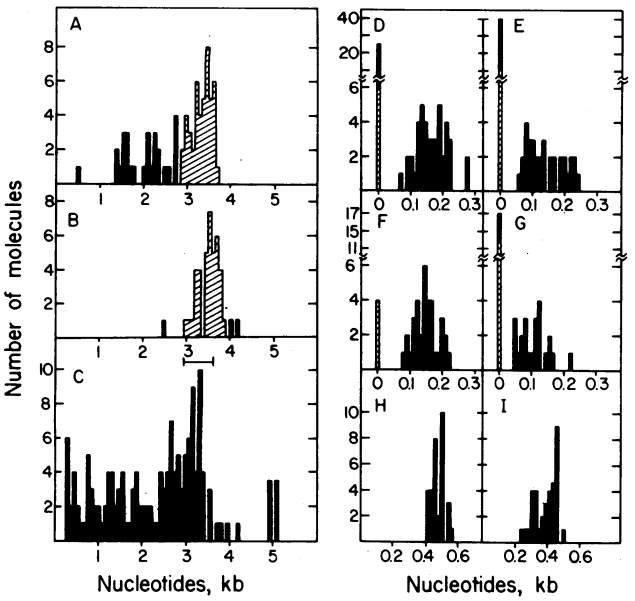

FIG. 5. Histograms of contour lengths of various parts of hexon mRNA and *Hin*dIII A DNA hybrids. kb is kilobases, 1000 bases or base pairs. *A* is a histogram of the contour length of the RNA·DNA duplex in R-loops of hexon mRNA and duplex *Hin*dIII A DNA. Similarly, *B* is a histogram of the contour length of RNA·DNA duplex in hybrids of hexon mRNA and single-stranded *Hin*dIII A DNA. An example of each of these types of hybrids is shown in *A* and *D*, respectively, of Fig. 4. In both *A* and *B* the hatched area represents hybrids found by intact RNA chains and these molecules were used in calculating average lengths of RNA·DNA duplex. *C* is the contour length histogram of the hexon mRNA as it is eluted from the gel. The molecules bracketed by the bar were assumed to be intact. *D* and *E* are the contour length histograms of the 5′ and 3′ single-stranded RNA tails, respectively, for the R-loop hybrids scored in *A*. Similar histograms for the 5′ and 3′ single-stranded RNA tails of the hybrids formed with hexon mRNA and single-stranded *Hin*dIII A DNA, respectively, are shown in *F* and *G*, respectively. A histogram of the duplex contour length between the end of the *Hin*dIII A DNA and the beginning of the R-loop hybrid is given in *H*. The histogram for the equivalent contour length between the end of the single-stranded *Hin*dIII A DNA and the beginning of the RNA·DNA hybrid region is shown in *I*. The hatched and solid areas scored on the 0 nucleotide position in *D* through *G* represent molecules falling in the hatched and solid areas, respectively, of *A* and *B*.

conditions. Therefore, single-stranded *Hin*dIII A DNA fragment was spread from a 50% formamide solution and visualized with the electron microscope. A histogram of the position of all hairpin structures relative to the nearest end of the single-stranded DNA segment was constructed for 51 molecules. No hairpin structures were observed at the map position of either end of the hexon mRNA (data not shown).

To ensure that the tails were linked to the hybrid by ribonuclease-sensitive bonds, hybrids were spread for visualization after treatment with pancreatic RNase under conditions where hybrid structures should be resistant to degradation. After RNase treatment, no 5′ or 3′ tails were observed, though the appropriate RNA·DNA hybrid length was seen when spread from an 80% formamide solution (data not shown).

If the sequences in the 5′ tail of hexon mRNA are transcribed upstream from the same template strand as the other 95% of the RNA sequences, then a hybrid of this mRNA and single-stranded *Eco*RI A DNA should form single-stranded DNA loops at the 5′ terminus of the duplex part of the hybrid. The single-stranded DNA forming the loop would correspond to the viral DNA sequences between the two regions of the template strand that were transcribed and joined during synthesis of the hexon mRNA. This experiment was performed and RNA·DNA hybrids of *Eco*RI A DNA and hexon mRNA were selected for scoring which, as expected, had a duplex region on one terminus terminating in a collapsed ball of single-stranded RNA. The R-loop data described in Fig. 1 predict that 70.9% of the hexon mRNA adjacent to the 5′ terminus should form hybrids with single-stranded *Eco*RI A DNA; the remaining 29.1% would be collapsed under these spreading conditions. An example of the RNA·DNA hybrids observed is shown in Fig. 4*G* and schematically in Fig. 4*H*. Data from 24 such structures were averaged for the following discussion. At the left end of the structure there is a single-stranded segment 5770 ± 390 bases (16.8% of the genome) in length followed by three deletion type loops of single-stranded DNA originating within 200 bases of the 5′ terminus of the RNA·DNA hybrid segment. The RNA·DNA hybrid has the expected contour length of 2710 ± 320 bases (7.74%). The order and contour length of the three loops from the left end of the genome to the right are: loop A, 1010 ± 130 (2.90%); loop B, 2350 ± 130 (6.70%); and loop C, 8060 ± 830 (23.0%). Loops A and B are separated by 80 ± 20 bases and loops B and C by 110 ± 10 bases. The simplest interpretation of this structure is that the 5′ tail of the hexon mRNA is composed of sequences transcribed from three different regions of the same strand of the viral DNA. The map positions of these three regions are 16.8 ± 1.1, 19.8 ± 1.1, and 26.9 ± 1.1. The segment of RNA·DNA hybrid at the 5′ terminus of the hexon mRNA creating loop A is too short to be distinguished in our electron micrographs. A comparison of the sum of the lengths of the duplex segments separating the three loops, 190 ± 30 bases, with the measured length of the 5′ tail on the hexon mRNA, 160 ± 50 bases, suggests that this region may be quite short. However, this segment would probably have to be at least 15 bases long to be stable under the denaturing conditions used for spreading these samples. Fifty single-stranded *Eco*RI A DNA molecules that contained one or more loops were scored from the same grid; no loop structures were observed that corresponded to the loops seen in the hexon mRNA/*Eco*RI A hybrids.

DISCUSSION

The most abundant viral mRNA found on the polyribosomes of cells 32 hr after infection with adenovirus 2 maps by the R-loop technique in the region of the genome that codes for the hexon polypeptide (12). When R-loops between this mRNA and the *Hin*dIII A fragment were examined in the electron microscope, almost all molecules containing an intact mRNA had single-stranded RNA tails of 160 nucleotides at their 5′ ends. To test whether this single-stranded 5′-end RNA tail was produced by branch migration forming homologous DNA·DNA base pairs, hybrids were formed between the purified mRNA and denatured *Hin*dIII A fragment DNA. A forked structure was observed at the 5′ end of this mRNA in almost all hybrids formed by the annealing of an intact mRNA chain to single-stranded DNA. This forked structure was observed under a variety of different conditions of mounting for visualization in the electron microscope and strongly suggests that a segment of the 5′ end of the mRNA is not complementary to the adjacent viral DNA sequences. The RNA sequences in each 5′ tail are apparently transcribed from the *r* strand of Ad2 DNA upstream from those coding for the body of the hexon mRNA. The structure of hexon mRNA and single-stranded *Eco*RI A DNA hybrids (see Fig. 4 *G* and *H*) suggests that RNA sequences of unknown length from 16.8 ± 1.1%, of 80 ± 20 bases from 19.8 ± 1.1%, and 110 ± 10 bases from 26.9 ± 1.1% are joined in the 5′ tail of hexon mRNA.

When total poly(A)-containing polyribosomal RNA was hybridized to denatured *Hin*dIII A under the same conditions, a second mRNA mapping in the region of the genome coding for the 100K polypeptide (12) was observed to have a similar forked structure at its 5′ terminus. Thus, a common short sequence of RNA might be attached to several late mRNAs. This is consistent with the observation of R. Gelinas, D. Klessig, and R. Roberts (personal communication) that a single T1 ribonuclease oligonucleotide containing a capped structure is found on total viral mRNAs isolated during the late stage of infection.

The three short segments forming the 5′ tail of hexon mRNA are probably spliced to the body of this mRNA during post-transcriptional processing. During the late stage of the lytic cycle the *r* strand of Ad2 is transcribed into long transcripts that originate in the left third of the genome and terminate near the right end (27–30). The region of the genome coding for the body of the hexon mRNA and the sequences in these three short RNA segments in the 5′ tail of this mRNA are probably included in this long transcript. Thus, a plausible model for the synthesis of the mature hexon mRNA would be the intramolecular joining of these short segments to the body of the hexon mRNA during the processing of a nuclear precursor to generate the mature mRNA. This would result in the maturation of one mRNA species from each longer precursor and would explain the large abundance of accumulated viral RNA sequences in the nucleus of cells during the late stage of the lytic cycle and the selective transport of certain viral RNA sequences to the cytoplasm (14). It is interesting to speculate on how general such a model for the processing of eukaryotic mRNAs could be. Assuming that eukaryotic mRNA sequences are adjacent to the 3′ terminus of heterogeneous nuclear RNA, this mechanism would certainly explain the observations by Perry and Kelley (31) that the 5′-terminal cap 1 structures of heterogeneous nuclear RNA from mouse cells are conserved during the processing of these sequences to cytoplasmic mRNAs, though the lengths of the RNA chains differ by a factor of 4 between these RNA fractions.

The role of the spliced RNA segment at the 5′ end of adenovirus late mRNA is subject to speculation. This RNA segment could be involved in the selection of certain viral RNA sequences for transport to the cell cytoplasm or could be responsible for the preferential translation of viral mRNA during the late stage of infection. Because the capped 5′ terminus of eukaryotic mRNA is thought to be directly involved in the initiation of translation of mRNA, an involvement of these sequences in the control of translation would be expected.

We would like to thank Arnold J. Berk, Timothy J. Harrison, Daniel Donoghue, and David Baltimore for comments on the manuscript, and Ms. Margarita Siafaca for typing the manuscript. We gratefully acknowledge the suggestion by David Baltimore that we map the RNA sequences in the 5′ tail by electron microscopy of RNA·DNA hybrids. This work was supported by an American Cancer Society Grant and career development support (VC-151A) to P.A.S., a Cancer Center Core Grant (CA-14051), and a National Institutes of Health Postdoctoral Fellowship to S.M.B. (CA02391-01).

1. Kates, J. (1970) *Cold Spring Harbor Symp. Quant. Biol.* **35**, 743–752.
2. Edmonds, M., Vaughan, M. H., Jr. & Nakazoto, H. (1971) *Proc. Natl. Acad. Sci. USA* **68**, 1336–1340.
3. Lee, S. Y., Mendecki, J. & Brawerman, G. (1971) *Proc. Natl. Acad. Sci. USA* **68**, 1331–1335.
4. Darnell, J. E., Jr., Wall, R. & Tushinski, R. J. (1971) *Proc. Natl. Acad. Sci. USA* **68**, 1321–1325.
5. Furuichi, Y., Morgan, M., Muthukrishnan, S. & Shatkin, A. J. (1975) *Proc. Natl. Acad. Sci. USA* **72**, 362–366.
6. Wei, C. M. & Moss, B. (1974) *Proc. Natl. Acad. Sci. USA* **71**, 3014–3018.
7. Philipson, L., Wall, R., Glickman, G. & Darnell, J. E. (1971) *Proc. Natl. Acad. Sci. USA* **68**, 2806–2809.
8. Hashimoto, S. & Green, M. (1976) *J. Virol.* **20**, 425–435.
9. Moss, B. & Koczot, F. (1976) *J. Virol.* **17**, 385–392.
10. Sharp, P. A. & Flint, S. J. (1976) *Current Topics in Microbiology and Immunology* **74**, 137–158.
11. Sharp, P. A., Gallimore, P. H. & Flint, S. J. (1974) *Cold Spring Harbor Symp. Quant. Biol.* **34**, 457–474.
12. Lewis, J., Atkins, J. F., Anderson, C., Baum, P. R. & Gesteland, R. F. (1975) *Proc. Natl. Acad. Sci. USA* **72**, 1344–1348.
13. Bachenheimer, S. & Darnell, J. E. (1975) *Proc. Natl. Acad. Sci. USA* **72**, 4445–4449.
14. Flint, S. J. & Sharp, P. A. (1976) *J. Mol. Biol.* **106**, 749–771.
15. Flint, S. J., Gallimore, P. H. & Sharp, P. A. (1975) *J. Mol. Biol.* **96**, 47–68.
16. Lindberg, U., Persson, T. & Philipson, L. (1972) *J. Virol.* **10**, 909–919.
17. Thomas, M., White, R. L. & Davis, R. W. (1976) *Proc. Natl. Acad. Sci. USA* **73**, 2294–2298.
18. Duesberg, P. H. & Vogt, P. K. (1973) *J. Virol.* **12**, 594–599.
19. Davis, R. W., Simon, M. & Davidson, N. (1971) in *Methods in Enzymology*, eds. Grossman, L. & Moldave, K. (Academic Press, New York), Vol. 21, pp. 413–428.
20. Casey, J. & Davidson, N. (1977) *Nucleic Acid Res.* **4**, 1539–1552.
21. Green, M. (1970) *Annu. Rev. Biochem.* **39**, 701–756.
22. White, R. L. & Hogness, D. S. (1977) *Cell* **10**, 177–192.
23. Westphal, H., Meyer, J. & Maizel, J. (1976) *Proc. Natl. Acad. Sci. USA* **73**, 2069–2071.
24. Chow, L. T., Roberts, J. M., Lewis, J. B. & Broker, T. M. (1977) *Cell*, in press.
25. Lee, C. S., Davis, R. W. & Davidson, N. (1970) *J. Mol. Biol.* **48**, 1–22.
26. Robberson, D., Aloni, Y., Attardi, G. & Davidson, N. (1971) *J. Mol. Biol.* **60**, 473–484.
27. Parsons, J. T. & Green, M. (1971) *Virology* **45**, 154–162.
28. Wall, R., Philipson, L. & Darnell, J. E. (1972) *Virology* **50**, 27–34.
29. McGuire, P. M., Swart, C. & Hodge, L. D. (1972) *Proc. Natl. Acad. Sci. USA* **69**, 1578–1582.
30. Goldberg, S., Weber, J. & Darnell, J. E. (1977) *Cell* **10**, 617–622.
31. Perry, R. P. & Kelley, D. E. (1976) *Cell* **8**, 433–442.